

# Dissolved iron anomaly in the deep tropical–subtropical Pacific: Evidence for long-range transport of hydrothermal iron

Jingfeng Wu<sup>a,\*</sup>, Mark L. Wells<sup>b</sup>, Robert Rember<sup>c</sup>

<sup>a</sup> *Rosenstiel School of Marine and Atmospheric Science, University of Miami, Miami, FL 33149, USA*

<sup>b</sup> *School of Marine Sciences, University of Maine, Orono, ME 04469, USA*

<sup>c</sup> *International Arctic Research Center, University of Alaska Fairbanks, Fairbanks, AK 99775, USA*

Received 26 February 2010; accepted in revised form 20 October 2010; available online 2 November 2010

## Abstract

Dissolved iron profiles along a north–south transect along 158°W in the tropical Pacific show evidence of two deepwater anomalies. The first extends from Station ALOHA (22.78°N) to the equator at ~1000–1500 m and lies below the maximum apparent oxygen utilization and nutrient (N, P) concentrations. The feature is not supported by vertical export processes, but instead corresponds with the lateral dilution field of  $\delta^3\text{He}$  derived from the Loihi seamount, Hawaii, though a sediment source associated with the Hawaiian Island Chain cannot be entirely ruled out. The second, deeper (2000–3000 m) anomaly occurs in tropical South Pacific waters (7°S) and also does not correlate with the depths of maximum nutrient concentrations or apparent oxygen utilization, but it does coincide closely with  $\delta^3\text{He}$  emanating from the East Pacific Rise, more than 5000 km to the east. We hypothesize that these anomalies represent the long-range (>2000 km) transport of hydrothermal iron residuals, stabilized against scavenging by complexation with excess organic ligands in the plume source regions. Such trace leakage of hydrothermal iron to distal plume regions would have been difficult to identify in most hydrothermal vent mapping studies because low analytical detection limits were not needed for the proximal plume regions. These findings suggest that hydrothermal activity may represent a major source of dissolved iron throughout the South Pacific deep basin today, as well as other regions having high mid-ocean spreading rates in the geologic past. In particular, we hypothesize that high spreading rates along the South Atlantic and Southern Ocean mid-oceanic ridges, combined with the upwelling ventilation of these distal hydrothermal plumes, may have increased ocean productivity and carbon export in the Southern Ocean. Assessing the magnitude and persistence of dissolved hydrothermal iron in basin scale deep waters will be important for understanding the marine biogeochemistry of iron and, potentially, on ocean productivity and climate change during the geologic past.

© 2010 Elsevier Ltd. All rights reserved.

## 1. INTRODUCTION

Increases in iron supply to open ocean surface waters are believed to have enhanced ocean primary production and effected global climate change during the geological past (e.g., Martin, 1990). Dust deposition is thought to be the primary factor regulating perturbations in iron supply over an otherwise persistent advective upwelling flux from the deep ocean. In large regions of the ocean,

particularly in the southern hemisphere where atmospheric dust loading is low, this upwelling flux is the predominant iron source to surface waters so changes in this flux have the potential to affect primary production, particularly in High Nitrate Low Chlorophyll regions. In the current paradigm deep ocean water iron concentrations are largely regulated by input from remineralization of sinking organic substrates and removal by particle scavenging (Wu and Boyle, 2002; Parekh et al., 2004), with iron-specific complexing ligands acting to buffer against removal of dissolved iron (Johnson et al., 1997). Superimposed on this vertically driven process is the lateral transport of iron from continental slopes (Martin et al., 1985;

\* Corresponding author. Tel.: +1 305 421 4714.  
E-mail address: [jwu@rsmas.miami.edu](mailto:jwu@rsmas.miami.edu) (J. Wu).

Landing and Bruland, 1987; Nishioka et al., 2007; Lam and Bishop, 2008), and subsurface advection of water along isopycnals from higher northern latitudes where aeolian inputs are greater (Measures et al., 2008). Hydrothermal vent systems are a point source largely ignored in this conceptual foundation, mainly because rapid precipitation of Fe(III) has been thought to highly restrict this enrichment to localized regions. The possibility that long-range transport of hydrothermal iron might create a residual halo influencing basin scale deepwater iron concentrations has not been systematically assessed by measuring the deep ocean distribution of dissolved Fe, although the influence of hydrothermal activity has been recently proposed by Boyle and Jenkins (2008) and examined by near-field Fe speciation studies (Bennett et al., 2008) and global ocean models (Tagliabue et al., 2010).

Sea floor hydrothermal activity has long been known to inject large amounts of iron into near-field mid-depth waters (Coale, 1991; Elderfield and Schultz, 1996; Field and Sherrell, 2000). The vast majority of reduced iron introduced with hydrothermal fluids is oxidized rapidly to Fe(III) species at concentrations that lie well above saturation in cold oxic seawater. This iron precipitates quickly as colloidal and particulate Fe(III) oxyhydroxides that deposit on the flanks of mid-ocean ridges proximal to the vent fields (Field and Sherrell, 2000). Indeed deep water dissolved iron distributions in the North Atlantic and North Pacific Oceans show nutrient-type profiles that are consistent with the export of iron-rich organic particles from surface waters and the subsequent release of this iron by microbial degradation of organic matter in the subsurface ocean (Johnson et al., 1997). However, this view has been shifting as new data accumulate on the vertical distribution of iron increase.

Boyle et al. (2005) identified an apparent anomaly of  $\sim 0.35$  nM dissolved iron in 1000 m depth waters at station

ALOHA (22.78°N, 158.00°W) north of Hawaii; i.e., an increase relative to waters above and below this depth. They suggested this apparent anomaly was generated by lateral advection of hydrothermally generated iron from the Loihi seamount  $\sim 500$  km to the southeast. This suggestion was based on the apparent correlation between Fe and  $\delta^3\text{He}$ , a tracer for hydrothermal fluid inputs (Lupton, 1998). Even so, it was not possible to entirely rule out alternate sources of this iron, including groundwater discharge from the Hawaiian islands (Moore et al., 2001).

In this paper, we present new dissolved iron data between 30°N and 7°S, along 140–158°W in the tropical/subtropical Pacific showing depth anomalies that are consistent with advective iron sources via long-range transport of hydrothermal iron from Loihi seamount and the hydrothermally active East Pacific Rise (EPR). These findings highlight the importance of better assessing the influence that hydrothermal systems might exert on the distribution of iron in deep ocean waters.

## 2. MATERIAL AND METHODS

Seawater samples were collected during the Wecoma WO503C cruise in April 2005 to the tropical Pacific. Nine vertical profiles from surface to 1000–4500 m depth were sampled along a transect beginning at station ALOHA (22°N, 158°W) extending southwards to  $\sim 7^\circ\text{S}$  along 158°W (Fig. 1). In addition, seawater samples were collected at SAFe Station 5 (30°N, 140°W) in October 2005. Water samples were collected using the ATE/vane sampler designed at the University of Alaska (Wu, 2007). Seawater samples were filtered through 0.4  $\mu\text{m}$  Nuclepore polycarbonate membranes within a few hours after sample collection. The sample filtrates were acidified to pH  $\sim 2$  with 2 ml Q-HCl (6 N, sub-boiling distilled in a quartz still, Fe blank is 1 nM/L HCl) per liter of seawater. The acidified

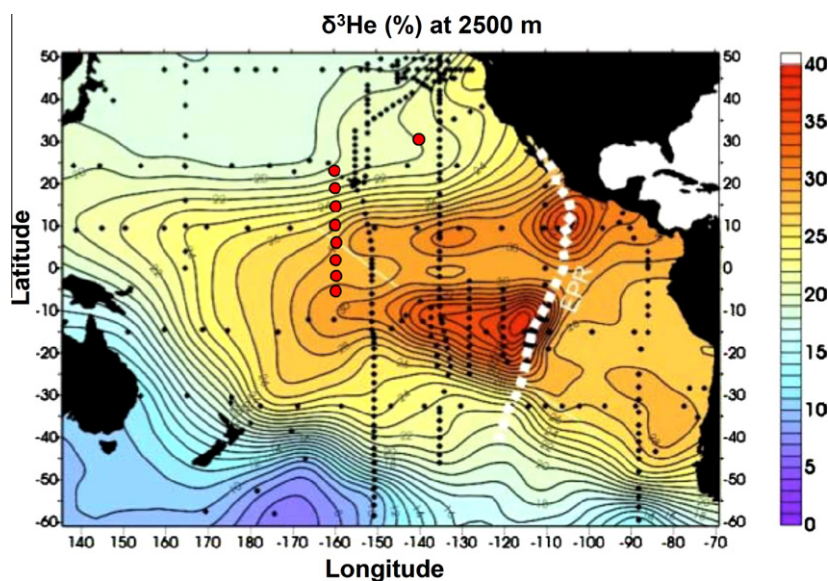


Fig. 1.  $\delta^3\text{He}$  distribution at 2500 m depth from the WOCE dataset with sampling station location shown as red filled circle. (For interpretation of the references to color in this figure legend, the reader is referred to the web version of this article.)

samples were stored in high-density polyethylene bottles at room temperature for more than 4 weeks before analysis.

Dissolved iron concentrations were measured after pre-concentration using a  $\text{Mg}(\text{OH})_2$  co-precipitation isotope dilution method (Wu and Boyle, 1997). Precipitates were analyzed by high resolution ICPMS (Finnigan MAT Element2) at the University of Alaska Fairbanks (Wu and Boyle, 1998). Detection limit for the method was  $\sim 0.03$  nM Fe with an average precision of  $\sim 10\%$  at 0.1 nM Fe. All sample handling and analyses were carried out using trace metal clean procedures (Wu and Boyle, 2002).

### 3. RESULTS

Vertical profiles of dissolved iron were measured along a southward section from the SAFe Station 5 ( $30^\circ\text{N}$ ,  $140^\circ\text{W}$ ) across the equator into the tropical South Pacific ( $7^\circ\text{S}$ ,  $158^\circ\text{W}$ ) (Figs. 1, 2A and Table 1). Dissolved iron concentrations increased with increasing depth at each station to a mid-depth maximum before decreasing toward the bottom. This mid-depth maximum was highest (0.9 nM) at  $\sim 1500$  m at  $22^\circ\text{N}$ ,  $158^\circ\text{W}$  and decreased with increasing distance to the north and south. The lens of elevated dissolved iron concentrations extended to  $5^\circ\text{N}$  and perhaps as far as the equator where the iron maximum was observed at  $\sim 2000$  m, well below that of the oxygen minimum and nitrate maximum (600 m) along this longitude ([www.ewoce.org](http://www.ewoce.org)). The peak in dissolved iron at  $\sim 1500$  m corresponds to elevated  $\delta^3\text{He}$  in this depth zone (Fig. 2B), which is indicative of the dispersal field of hydrothermal vent fluids from the Loihi seamount situated  $\sim 400$  km to the southeast of  $22^\circ\text{N}$ ,  $158^\circ\text{W}$  (Lupton, 1998; Malahoff et al., 2006). The  $\delta^3\text{He}$  distribution from Loihi dissipates almost due eastwards but its margin extends northwards beyond  $30^\circ\text{N}$  and southwards as far as  $5^\circ\text{N}$ ,  $\sim 2300$  km to the south of Loihi in this section (Fig. 2B).

In addition to the iron maximum at 1500 m in the northern section of this transect, there also is a previously unreported iron maximum situated between 2000 and 3000 m in the southern portion of the transect (Fig. 2A). The broad iron maximum at  $7^\circ\text{S}$  lies  $\sim 2000$  m below the nitrate maximum, dissolved oxygen minimum, and the depth of maximum AOU ( $\sim 300$ – $500$  m, Fig. 3). Overlapping these iron data with those reported by Johnson et al. (1997) at  $3^\circ\text{S}$ ,  $140^\circ\text{W}$  suggests that the maximal dissolved iron concentration occurs at  $\sim 2400$  m in this region, bracketed above and below this depth by symmetrically decreasing concentrations.

The mid-depth iron maximum in equatorial waters also shows a spatial relationship with  $\delta^3\text{He}$  (Fig. 2C). This close relationship is apparent at  $7^\circ\text{S}$ , where the peak in dissolved iron concentrations shown here and in Johnson et al. (1997) matches almost exactly the peak of  $\delta^3\text{He}$  at 2400 m depth (Figs. 2C and 3). The profile at this station lies on the northern margin of the  $\delta^3\text{He}$  tongue that extends eastwards  $\sim 5300$  km to the extensive hydrothermal vent plume at 2500 m above the East Pacific Rise (EPR) ( $15^\circ\text{S}$ ,  $110^\circ\text{W}$ ) (Fig. 1); the most active spreading center along the Pacific mid-oceanic ridge system (Lupton, 1998).

### 4. DISCUSSION

The markedly higher dissolved iron concentrations between 1000 and 2000 m at Station ALOHA ( $22.78^\circ\text{N}$ ,  $158.0^\circ\text{W}$ ) has been reported previously (Boyle et al., 2005), and the findings here extend the unique signature of this iron anomaly (Fig. 2A). Boyle et al. (2005) suggested this feature resulted from lateral iron input due to hydrothermal activity at the Loihi seamount located  $\sim 500$  km to the southeast. A lens of elevated dissolved iron appears to spread to the north(east) and south at this depth range, decreasing in concentration with distance from Station ALOHA (Fig. 1). The iron gradient lies below the maxima for N, P (at  $\sim 1000$  m) and the oxygen minimum zone (at  $\sim 600$  m) in this region ([www.ewoce.org](http://www.ewoce.org)), suggesting that the elevated iron concentrations are not explained by the remineralization of sinking organic matter. While lateral transport and dilution of hydrothermal fluids from Loihi predominantly are eastwards, based on  $\delta^3\text{He}$  distribution (Lupton, 1998), the southern margin of this mixing plume appears to extend towards the equator (Fig. 2B). Differences in sampling depths of the  $\delta^3\text{He}$  and dissolved iron datasets preclude a direct quantitative comparison, but the correspondence suggests that the lens of elevated dissolved iron concentrations at 1000–1500 m depth north of the equator along  $158^\circ\text{W}$  may result from longer-range transport of hydrothermally derived iron, although contributions from lateral advection of sediment derived iron from the Hawaiian Islands (e.g., Lam and Bishop, 2008) cannot be completely ruled out.

Better evidence for the long-range transport of hydrothermal iron is seen in S. Pacific waters, where a second iron anomaly observed at  $\sim 2500$  m depth at  $7^\circ\text{S}$  lies far ( $\sim 2000$  m) below the nutrient (N, P) maxima (Figs. 2A and 3). The strong decoupling of Fe, N and P is surprising because good correlations among these parameters with depth have been observed in the North Atlantic and North Pacific Oceans (Johnson et al., 1997; Wu et al., 2001). If the vertical distribution of iron reflects a steady state balance of remineralization and scavenging by sinking particles, we can estimate to a first order the broad shape of an iron profile dominated by regeneration using the parameter AOU, the amount of oxygen consumed by organic matter remineralization, and a ratio of  $\sim 1.5$   $\mu\text{mol Fe:mol C}$  in organic matter (Sunda, 2002) (Fig. 3), although the calculation does not account for particle scavenging. The estimates correlate reasonably well in near surface ( $< 500$  m) waters, but not in deeper waters, with the measured dissolved iron peak at  $\sim 2500$  m being substantially deeper than the calculated regenerated iron maximum at 500–800 m depth (Fig. 3). This discrepancy is in contrast to measured iron distributions in the North Atlantic and North Pacific Oceans (Martin et al., 1987, 1993), which match AOU-derived distributions using cellular Fe:C ratios of 2–13  $\mu\text{mol Fe:mol C}$  (Sunda and Huntsman, 1995; Johnson et al., 1997). Although higher Fe:C ratios would yield the observed mid-depth iron concentrations measured here, substantially higher scavenging rates or a much lower Fe:C ratio for the near surface waters would be required before the model profile would approach that observed; a unique

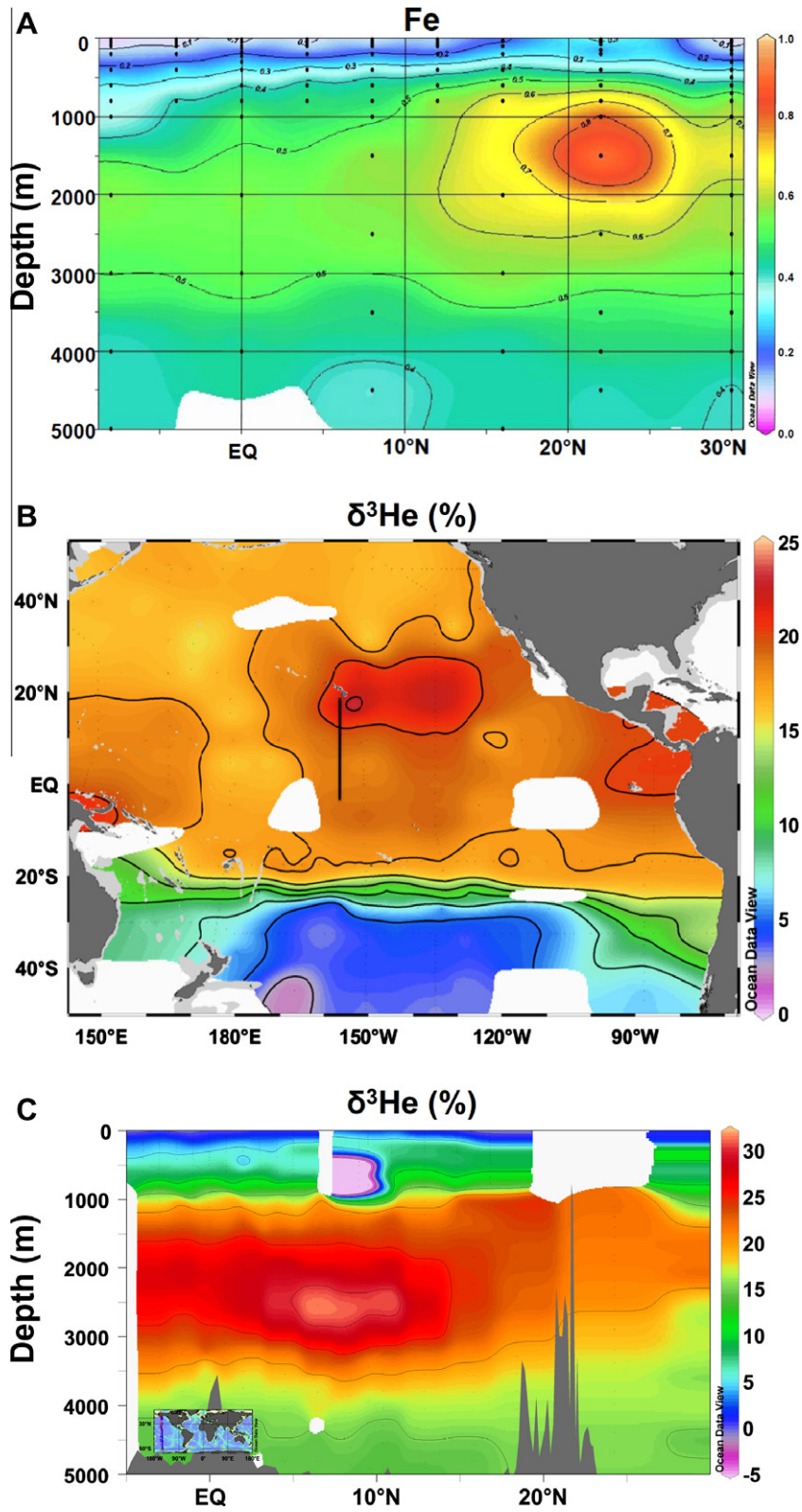


Fig. 2. (A) Dissolved iron distribution at 140–158°W in the tropical North Pacific in October 2004–April 2005. The 30°N station was at 140°W, SAFE Station 5, sampled in October 2004. (B) The distribution of  $\delta^3\text{He}$  showing the dispersal plume of hydrothermal fluid at 1200 m depth. (C) The distribution of  $\delta^3\text{He}$  showing the dispersal plume of hydrothermal fluid at 2000–3000 m in the tropical Pacific.

Table 1

Data table for Fig. 2A. The samples for profile at 30°N, 140°W were collected in October 2004 during SAFE cruise and the rest of samples were collected in April 2005 during WOC305 cruise.

Longitude	Latitude	Depth (m)	<0.4 $\mu\text{m}$ Fe (nM)
140°W	30°N	25	0.025
		30	0.057
		50	0.065
		100	0.083
		150	0.075
		200	0.099
		300	0.236
		400	0.346
		500	0.346
		600	0.425
		700	0.605
		800	0.693
		1000	0.634
		1500	0.665
		2000	0.559
		2500	0.589
		158°W	22°N
30	0.363		
50	0.341		
75	0.144		
150	0.0953		
200	0.22		
400	0.341		
600	0.589		
800	0.753		
1000	0.858		
1500	0.864		
158°W	16°N	30	0.116
		100	0.212
		200	0.311
		400	0.485
		600	0.607
		800	0.77
		2000	0.633
		3000	0.563
		4000	0.408
		5000	0.374
158°W	12°N	15	0.086
		50	0.11
		75	0.073
		100	0.0602
		200	0.206
		400	0.431
		600	0.517
		800	0.669
158°W	8°N	15	0.0417
		30	0.069

Table 1 (continued)

Longitude	Latitude	Depth (m)	<0.4 $\mu\text{m}$ Fe (nM)		
		50	0.0577		
		75	0.09		
		100	0.102		
		200	0.385		
		400	0.481		
		600	0.503		
		800	0.433		
		1000	0.472		
		1500	0.587		
		2500	0.547		
		3500	0.444		
		4500	0.357		
		158°W	4°N	15	0.076
				30	0.046
50	0.078				
75	0.066				
100	0.056				
200	0.194				
400	0.481				
600	0.501				
158°W	0°N	800	0.494		
		15	0.0226		
		30	0.0227		
		50	0.0359		
		100	0.0394		
		125	0.0515		
		175	0.1716		
		200	0.334		
		225	0.349		
		300	0.316		
158°W	4°S	400	0.394		
		600	0.486		
		800	0.473		
		1000	0.546		
		2000	0.542		
		3000	0.516		
		4000	0.371		
		15	0.0428		
		30			
		50	0.0405		
158°W	7°S	75	0.058		
		100	0.074		
		200	0.201		
		400	0.411		
		800	0.452		
		15	0.043		
		30	0.0588		
		75	0.066		
		100	0.0505		
		200	0.17		
		400	0.263		
		600	0.342		
		800	0.366		
		1000	0.398		
		2000	0.498		
		3000	0.501		
		4000	0.399		
		5000	0.405		

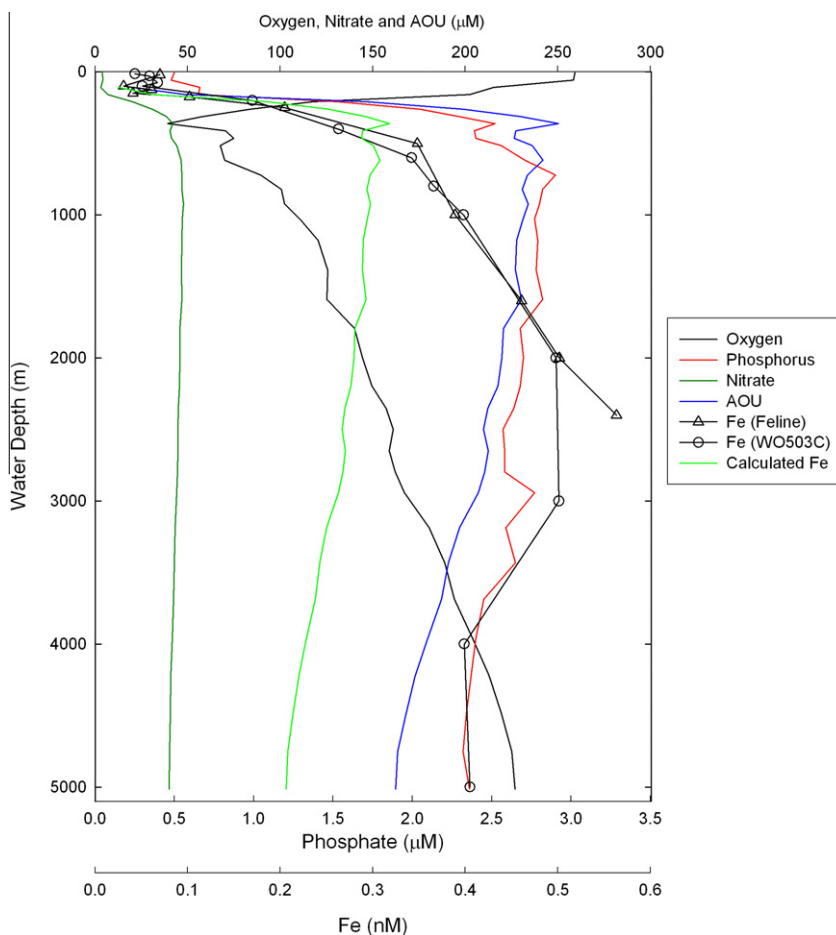


Fig. 3. Vertical profiles of dissolved iron at 7°S, 158°W. Published iron data for this region (Feline, Johnson et al., 1997) are shown for comparison. Shown also is the estimated steady state vertical distribution of iron that would be supported by remineralization of sinking particles having an Fe:C ratio of 1.5  $\mu\text{mol/mol}$ , and the vertical profiles of oxygen, AOU and nitrate measured by the WOCE program at 6°S, 152°W.

parameterization relative to other ocean regions. Although low rates of aeolian Fe input to the tropical region may result in a lower Fe:C ratio for the organic matter sinking from the euphotic zone, such particle flux would need to have a high Fe:C ratio to account for the Fe maxima in the deep water. Alternatively, it is conceivable that a deep-water “excess” of dissolved iron might arise if a portion of the carbon export was associated with faster sinking particulates that preferentially release iron relative to carbon in mid-depth waters; for example, a diatom-enhanced flux. But such fast sinking particulate flux has not been reported for the contemporary tropical oceans. Other explanations are required to account for this deepwater iron anomaly.

The EPR is one of the most active hydrothermal systems of the world oceans, and  $\delta^3\text{He}$  anomalies that reflect inputs of these hydrothermal fluids occur throughout most mid-depth waters of the South Pacific Ocean (Lupton, 1998; Fig. 1). The vast majority of iron released from hydrothermal vents rapidly oxidizes in the cold seawater, precipitates as colloidal and particulate Fe(III) oxyhydroxides, and deposits along the ridge flanks proximal to the vent fields. The result is a rather concentrated distribution of “excess”

particulate iron around and downstream of active vents that is used both to locate and map vent fields (Coale et al., 1991; Elderfield and Schultz, 1996; Field and Sherrell, 2000) as well as to estimate plume dispersion rates from the oxidation kinetics of hydrothermally released Fe(II) (Statham et al., 2005). However, there has been little consideration given to the potential far-field impacts of hydrothermal vent activity, the perception being that deep water dissolved iron concentrations instead are controlled by surface export and particle scavenging processes (Johnson et al., 1997). But this perspective recently has been challenged by iron isotopic data in ocean sediments that indicate that hydrothermal iron inputs could account for a significant fraction of the dissolved iron pool in the deep ocean (Chu et al., 2006).

Mid-depth waters in the Pacific Ocean appear to contain a persistent  $\sim 2$  nM excess of strong, metal-specific Fe(III)-complexing organic ligands, similar in strength to the weaker ligand class seen in surface waters (Rue and Bruland, 1995). In principle then, the mixing of seawater and hydrothermal fluids in the proximal plume would result in a small fraction of hydrothermal iron being complexed

and stabilized against particle scavenging. This small residual almost certainly would not be observed during most mapping studies of hydrothermal plumes because these concentrations lie about an order of magnitude below the detection limits of many analytical methods used during mapping and vent characterization studies (e.g., Coale et al., 1991; Statham et al., 2005). Although the specific source and turnover rates of these organic ligands are not understood, their ubiquitous presence in deep ocean waters provides a mechanism by which hydrothermally derived iron could be transported thousands of kilometers by deep ocean currents. Indeed the comparison of dissolved iron and  $\delta^3\text{He}$  vertical distributions at  $7^\circ\text{S}$  shows a remarkable degree of correspondence, with both maxima at 2000–3000 m depth (Fig. 4). These data suggest that the far-field transport of hydrothermal iron may be on the order of at least 5000 km. Recent deepwater iron measurements by Boyle and Jenkins (2008) in the western S. Pacific ( $20^\circ\text{S}$ ,  $170^\circ\text{W}$ ) also suggest that the hydrothermal residuals in this vent plume may survive long-range transport from its source region on the EPR. Measurements of dissolved Fe speciation near hydrothermal plumes using competitive ligand exchange–cathodic stripping voltammetry (CLE–CSV) showed that the observed Fe-binding organic ligand concentrations are high enough to account for stabilization of  $\sim 4\%$  of the total Fe emitted from the  $5^\circ\text{S}$  vent sites (Bennett et al., 2008).

Even so, it remains possible that the observed iron peak in the tropical south Pacific results more from the layering of water masses containing preformed iron advected from other regions; e.g., shallow waters from iron-deplete high latitude South Pacific combined with lower aeolian inputs

to the surface ocean generating lower dissolved iron concentrations in the upper 1000 m of the water column in the South Pacific as compared to those in the North Pacific and North Atlantic Oceans. If non-hydrothermal preformed iron is responsible for the mid-depth iron peak at  $7^\circ\text{S}$ , dissolved iron concentrations in the high latitude surface waters to the south that ventilate the mid-depth (2000–3000 m) south Pacific Ocean would necessarily be higher than the northerly and southerly surface waters ventilating depths above and below 2500 m. Such a dissolved iron distribution is unlikely to occur in the near surface waters in the high latitude South Pacific Ocean/Southern Ocean given a lack of obvious iron sources to these waters. Alternatively, the deepwater iron anomaly conceivably might reflect a residual from the lateral transport of iron from the South American continent (Landing and Bruland, 1987; Elrod et al., 2004; Lam and Bishop, 2008). Although dissolved iron profiles from the eastern (opposite) side of the EPR are not available to test this hypothesis, it seems unlikely that this transport would selectively inject iron at only 2000–3000 m depth.

It is worth noting the mid-depth iron maximum at  $7^\circ\text{S}$  has a striking similarity to iron profiles below 500 m in the South Atlantic ( $25.5^\circ\text{S}$ ,  $37.0^\circ\text{W}$ ) where hydrothermal activity is minimal (Bergquist et al., 2007). Although the Bergquist et al. (2007) deep water maximum at 2000–3000 m also cannot be explained by vertical particle flux from surface waters at this site, they conclude that it reflects the southward advection of North Atlantic Deep Water enriched with iron from Saharan dust deposition in the North Atlantic. If so, then both studies suggest the potential for long-range transport of iron from “point” type sources,

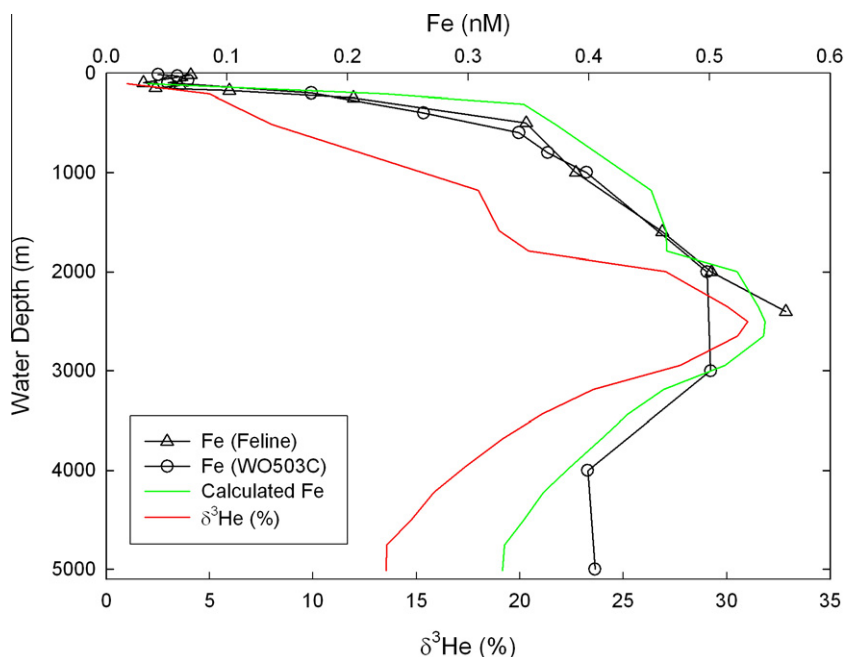


Fig. 4. A comparison between the dissolved iron profile measured at  $7^\circ\text{S}$ ,  $158^\circ\text{W}$  and  $\delta^3\text{He}$  measured by WOCE program at  $6^\circ\text{S}$ ,  $152^\circ\text{W}$ . Also shown is an estimated dissolved iron profile calculated based on the sum of contributions from the remineralization of sinking organic matter with an Fe:C ratio of  $1.5 \mu\text{mol/mol}$ , and hydrothermal iron contribution estimated based on an Fe:He ratio of  $0.009 \text{ nM}/\%$  (see text).

whether from vertical plumes of sinking dust particles, or lateral plumes from hydrothermal vents.

The potential significance of hydrothermal transport to basin scale iron biogeochemistry in the Pacific can be roughly estimated. Assuming that the lateral advection of preformed iron from shallow water is not significant the vertical distribution of dissolved iron at 7°S can be reasonably fitted using a combination of iron regeneration from the remineralization of sinking organic matter (1.5  $\mu\text{mol Fe/mol C}$ ) and an additional hydrothermal iron input (Fe:  $\delta^3\text{He}$  ratio = 0.009 nM/%) (Fig. 4). If iron scavenging is ignored, the upper limit for the hydrothermal contribution to deepwater iron concentrations can be estimated using this Fe:  $\delta^3\text{He}$  ratio and the  $\delta^3\text{He}$  distribution in the Pacific (Fig. 1). In this case, the distal dispersion of hydrothermal iron from the EPR might account for as much as 40–50% of total dissolved iron concentrations between 1000 and 5000 m depth in the tropical Pacific. Although the actual contributions likely will be less due to the effects of long term scavenging of organically complexed iron, this estimate is higher than the 12–22% suggested by Bennett et al. (2008) for the global ocean based on CLE–CSV Fe speciation measurements near a hydrothermal plume, but it falls within the range (0.2–0.5 nM) of dissolved Fe anomaly modeled for the South Pacific by Tagliabue et al. (2010).

Present day spreading rates are highest along the East Pacific Rise, but this has not always been the case (e.g., Cogné and Humler, 2006). If indeed dissolved Fe in the South Pacific (Fig. 2A) is derived from hydrothermal sources, it is possible that the increased hydrothermal activities during the geological past along the South Atlantic, Southeast and Southwest Indian, and Pacific Antarctic spreading ridges also would have generated residual hydrothermal dissolved iron in mid-depth waters. If this iron was sufficiently persistent, upwelling ventilation of the distal plume waters in the Southern Ocean may have influenced ocean productivity in this globally important, iron limited region as proposed by the recent modeling work of Tagliabue et al. (2010). A more quantitative evaluation of this potential contribution awaits more detailed study of the distribution, size fractionation, isotopic composition, and reactivity of dissolved iron and iron complexing organic ligands in Pacific deep waters.

## REFERENCES

- Bennett S. A., Achterberg E. P., Connelly D. P., Statham P. J., Fones G. R. and German C. R. (2008) The distribution and stabilization of dissolved Fe in deep-sea hydrothermal plumes. *Earth Planet. Sci. Lett.* **65**, 157–167.
- Bergquist R. A., Wu J. F. and Boyle E. A. (2007) Variability in oceanic dissolved iron is dominated by the colloidal fraction. *Geochim. Cosmochim. Acta* **71**, 2960–2974.
- Boyle E. A. and Jenkins W. (2008) Goldschmidt abstracts 2008. *Geochim. Cosmochim. Acta* **72**(12, Suppl. 1), A107.
- Boyle E. A., Bergquist R. A., Hayser R. A. and Mahowald N. (2005) Iron, manganese, and lead at Hawaii ocean time-series station ALOHA: temporal variability in an intermediate water hydrothermal plume. *Geochim. Cosmochim. Acta* **69**, 933–952.
- Chu N. C. et al. (2006) Evidence for hydrothermal venting in Fe isotope compositions of the deep Pacific Ocean through time. *Earth Planet. Sci. Lett.* **245**, 202–217.
- Coale K. H. (1991) Effects of iron, manganese, copper, and zinc enrichments on productivity and biomass in the subarctic Pacific. *Limnol. Oceanogr.* **36**, 1851–1864.
- Coale K. H., Chin C. S., Massoth G. J., Johnson K. S. and Baker E. T. (1991) In-situ chemical mapping of dissolved iron and manganese in hydrothermal plumes. *Nature* **352**, 325–328.
- Cogné J. P. and Humler E. (2006) Trends and rhythms in global seafloor generation rate. *Geochem. Geophys. Geosyst.* **7**. doi:10.1029/2005GC001148.
- Elderfield H. and Schultz A. (1996) Mid-ocean ridge hydrothermal fluxes and the chemical composition of the ocean. *Annu. Rev. Earth Planet. Sci.* **24**, 191–224.
- Elrod V. A., Berelson W. M., Coale K. H. and Johnson K. S. (2004) The flux of iron from continental shelf sediments: a missing source for global budgets. *Geophys. Res. Lett.* **31**. doi:10.1029/2004GL02021.
- Field M. P. and Sherrell R. M. (2000) Dissolved and particulate Fe in a hydrothermal plume at 9°45'N, East Pacific Rise: slow Fe (II) oxidation kinetics in Pacific plumes. *Geochim. Cosmochim. Acta* **64**, 619–628.
- Johnson K. S., Gordon R. M. and Coale K. H. (1997) What controls dissolved iron concentrations in the world ocean? *Mar. Chem.* **57**, 137–161.
- Lam P. J. and Bishop J. K. B. (2008) The continental margin is a key source of iron to the HNLC North Pacific Ocean. *Geophys. Res. Lett.* **35**. doi:10.1029/2008GL033294.
- Landing W. M. and Bruland K. W. (1987) The contrasting biogeochemistry of iron and manganese in the Pacific Ocean. *Geochim. Cosmochim. Acta* **51**, 29–43.
- Lupton J. (1998) Hydrothermal helium plumes in the Pacific Ocean. *J. Geophys. Res.* **103**, 15853–15868.
- Malahoff A., Kolotyrkina I. Y., Midson B. P. and Massoth G. J. (2006) A decade of exploring a submarine intraplate volcano: hydrothermal manganese and iron at Loihi volcano, Hawaii. *Geochem. Geophys. Geosyst.* **6**. doi:10.1029/2005GC001222.
- Martin J. H. (1990) Glacial–Interglacial CO<sub>2</sub> change: the iron hypothesis. *Paleoceanography* **5**, 1–13.
- Martin J. H., Knauer G. A. and Broenkow W. W. (1985) VERTEX: lateral transport of manganese in the northeast Pacific. *Deep Sea Res. Part A* **32**, 1405–1427.
- Martin J. H., Knauer G. A., Karl D. M. and Broenkow W. (1987) VERTEX: carbon cycling in the Northeast Pacific. *Deep Sea Res. Part A* **34**, 267–285.
- Martin J. H., Fitzwater S. E., Gordon R. M., Hunter C. N. and Tanner S. J. (1993) Iron, primary production and carbon–nitrogen flux studies during the JGOFS North Atlantic Bloom Experiment. *Deep Sea Res.* **40**, 115–134.
- Measures C. I., Landing W. M., Brown M. T. and Buck C. S. (2008) High-resolution Al and Fe data from the Atlantic Ocean CLIVAR–CO<sub>2</sub> Repeat Hydrography A16N transect: extensive linkages between atmospheric dust and upper ocean geochemistry. *Global Biogeochem. Cycles* **22**. doi:10.1029/2007GB003042.
- Moore W. S., Pauli C. K. and Ussle W. (2001) Short-lived radium isotopes in the Hawaiian Margin: evidence of large fluid fluxes through the Puna Ridge. In *American Geophysical Union Fall Meeting*. #OS42E-10 (abstr.).
- Nishioka J. et al. (2007) Iron supply to the western subarctic Pacific: importance of iron export from the Sea of Okhotsk. *Geophys. Res. Lett.* **112**. doi:10.1029/2006JC004055.
- Parekh P., Follows M. and Boyle E. A. (2004) Modeling the global ocean iron cycle. *Global Biogeochem. Cycles* **18**. doi:10.1029/2003GB002061.
- Rue E. L. and Bruland K. W. (1995) Complexation of iron(III) by natural organic ligands in the central North Pacific as determined by a new competitive ligand equilibration/ adsorptive

- cathodic stripping voltammetric method. *Mar. Chem.* **50**, 117–139.
- Statham P. J., German C. R. and Connelly D. P. (2005) Iron(II) distributions and oxidation kinetics in hydrothermal plumes and the Kairei and Edmond vent sites, Indian Ocean. *Earth Planet. Sci. Lett.* **236**, 588–596.
- Sunda W. G. (2002) Bioavailability and bioaccumulation of iron in the sea. In *The Biogeochemistry of Iron in Seawater* (eds. D. R. Turner and K. A. Hunter). John Wiley & Sons.
- Sunda W. G. and Huntsman S. A. (1995) Iron uptake and growth limitation in oceanic and coastal phytoplankton. *Mar. Chem.* **50**, 189–206.
- Tagliabue A. et al. (2010) Hydrothermal contribution to the oceanic dissolved iron inventory. *Nat. Geosci.* **3**, 252–256.
- Wu J. (2007) Determination of picomolar iron in seawater by double  $Mg(OH)_2$  precipitation isotope dilution high resolution ICPMS. *Mar. Chem.* **103**, 370–381.
- Wu J. and Boyle E. A. (1997) Low blank preconcentration technique for the determination of lead, copper, and cadmium in small-volume seawater samples by isotope dilution ICPMS. *Anal. Chem.* **69**, 2464–2470.
- Wu J. and Boyle E. A. (1998) Determination of iron in seawater by high resolution isotope dilution inductively coupled mass spectrometry after  $Mg(OH)_2$  coprecipitation. *Anal. Chim. Acta* **367**, 183–191.
- Wu J. and Boyle E. A. (2002) Iron in the Sargasso Sea: implications for the processes controlling dissolved Fe distribution in the ocean. *Global Biogeochem. Cycles* **16**. doi:10.1029/2001GB001453.
- Wu J. F., Boyle E. A., Sunda W. G. and Wen L.-S. (2001) Soluble and colloidal iron in the oligotrophic North Atlantic and North Pacific. *Science* **293**, 847–849.

Associate editor: Robert H. Byrne